

# Gas-Phase Purification of Single-Wall Carbon Nanotubes

John L. Zimmerman, Robert Kelley Bradley, Chad B. Huffman,  
Robert H. Hauge, and John L. Margrave\*

Department of Chemistry, Rice Quantum Institute, and the Center for Nanoscale Science and  
Technology, Rice University, Houston, Texas 77005

Received November 1, 1999. Revised Manuscript Received February 21, 2000

A gas-phase purification method for raw nanotube material has been developed which incorporates a chlorine, water, and hydrogen chloride gas mixture to remove unwanted carbon. The evolved gases can be easily monitored by infrared spectroscopy to follow the cleaning process. The quality of the final material was verified by SEM (scanning electron microscopy), TGA (thermogravimetric analysis), and UV–vis (ultraviolet and visible absorption spectroscopy). The yield of ~15 wt % indicates a uniquely selective carbon surface chemistry that prevents etching of the nanotubes, which are generally more reactive due to their larger curvature. Although the technique's usefulness for large-scale purification was not determined, the ability to purify single-wall nanotubes by a gas-phase method has been demonstrated, and a mechanism proposed.

## Introduction

Single-wall nanotubes, which are graphitic tubes approximately a nanometer in diameter, were first discovered by S. Iijima, and have since been produced by pulsed laser vaporization, arc discharge, or chemical vapor deposition.<sup>1–4</sup> The proposed future applications of this unique material include high-strength composites, molecular electronics, nanoprobe, energy storage or conversion, and many others.<sup>5</sup> The research directed at these applications will require pure samples for physical and chemical processing. The highest synthetic yield, of greater than ~70 vol % nanotubes, was obtained by the pulsed laser process in a 1 in. furnace. However, the scale-up of this method to a 4 in. furnace resulted in lower quality material, and thus a greater need for purification.

The procedures used thus far for single-wall nanotube purification rely on some type of ultracentrifugation (UCF) or filtration, including microfiltration, ultrasonically assisted filtration, or cross-flow filtration (CFF).<sup>6,7</sup> The most recently developed technique uses an oxidizing-acid reflux of the raw material, known as felt, followed by UCF. The separation in this case uses the difference in water solubility between the small-oxygenated carbon species and the nanotubes.<sup>8</sup> The other

common procedure uses CFF in place of the centrifugation. Although the acid treatment breaks up the unwanted carbon, the actual separation is done by the CFF and is based on physical size and aspect ratio.<sup>9</sup>

Although multiwall nanotubes can be purified by a variety of gas-phase oxidations, the use of a chemical purification process has not been demonstrated for single-wall nanotubes. Multiwall nanotubes have been purified by oxygen, a combination of copper and oxygen, or a combination of bromine and oxygen.<sup>10–13</sup> The copper and bromine are intended to serve as intercalates, and the resulting difference in oxidation rate is used to burn off the unwanted carbon. The difference in oxidation behavior is more pronounced with the intercalate present and results in higher yields. Attempts to use similar procedures for single-wall nanotubes resulted in tube destruction. For example, using the bromine and oxygen system the yield was ~3 wt %. This is related to the amount of curvature experienced by the graphite sheet. Therefore, the oxidation resistance of single-wall nanotubes is less than that of multiwall nanotubes, which are in turn less resistant than large carbon fibers. This would seem to preclude chemical purification for single-wall tubes, but we show here that the correct conditions allow for removal of amorphous carbon or onionated particles, with or without metal catalyst inside, while simultaneously protecting the nanotubes.

(1) Iijima, S. *Nature* **1991**, *354*, 56.  
(2) Thess, A.; Lee, R.; Nikolaev, P.; Dai, H.; Petit, P.; Robert, J.; Xu, C.; Lee, Y. H.; Kim, S. G.; Rinzler, A. G.; Colbert, D. T.; Scuseria, G. E.; Tomanek, D.; Fischer, J. E.; Smalley R. E. *Science* **1996**, *273*, 483.  
(3) Journet, C.; Maser, W. K.; Bernier, P.; Loiseau, A.; Lamy de la Chapelle, M.; Lefrant, S.; Deniard, P.; Lee, R.; Fischer, J. E. *Nature* **1997**, *388*, 756.  
(4) Kong, J.; Cassell, A. M.; Dai, H. *Chem. Phys. Lett.* **1998**, *292*, 567.  
(5) Ajayan, P. M. *Chem. Rev.* **1999**, *99*, 1787.  
(6) Bandow, S.; Rao, A. M.; Williams, K. A.; Thess, A.; Smalley, R. E.; Eklund, P. C. *J. Phys. Chem. B* **1997**, *101*, 8839.  
(7) Shelimov, K. B.; Esenaliev, R. O.; Rinzler, A. G.; Huffman, C. B.; Smalley, R. E. *Chem. Phys. Lett.* **1998**, *282*, 429.

(8) Huffman, C. B.; Harris, L. C. Unpublished results, Rice University, 1999.  
(9) Rinzler, A. G.; Liu, J.; Dai, H.; Nikolaev, P.; Huffman, C. B.; Rodriguez-Macias, F. J.; Boul, P. J.; Lu, A. H.; Heymann, D.; Colbert, D. T.; Lee, R. S.; Fischer, J. E.; Rao, A. M.; Eklund, P. C.; Smalley, R. E. *Appl. Phys. A* **1998**, *67*, 29.  
(10) Ebbesen, T. W.; Ajayan, P. M.; Hiura, H.; Tanigaki, K. *Nature* **1994**, *367*, 519.  
(11) Ikazaki, F.; Ohshima, S.; Uchida, K.; Kuriki, Y.; Hayakawa, H.; Yumura, M.; Takahashi, K.; Tojima, K. *Carbon* **1994**, *32–8*, 1539.  
(12) Chen, Y. K.; Green, M. L. H.; Griffin, J. L.; Hammer, J.; Lago, R. M.; Tsang, S. C. *Adv. Mater.* **1996**, *8–12*, 1012.  
(13) Morishita, K.; Takarada, T. *J. Mater. Sci.* **1999**, *34(6)*, 1169.

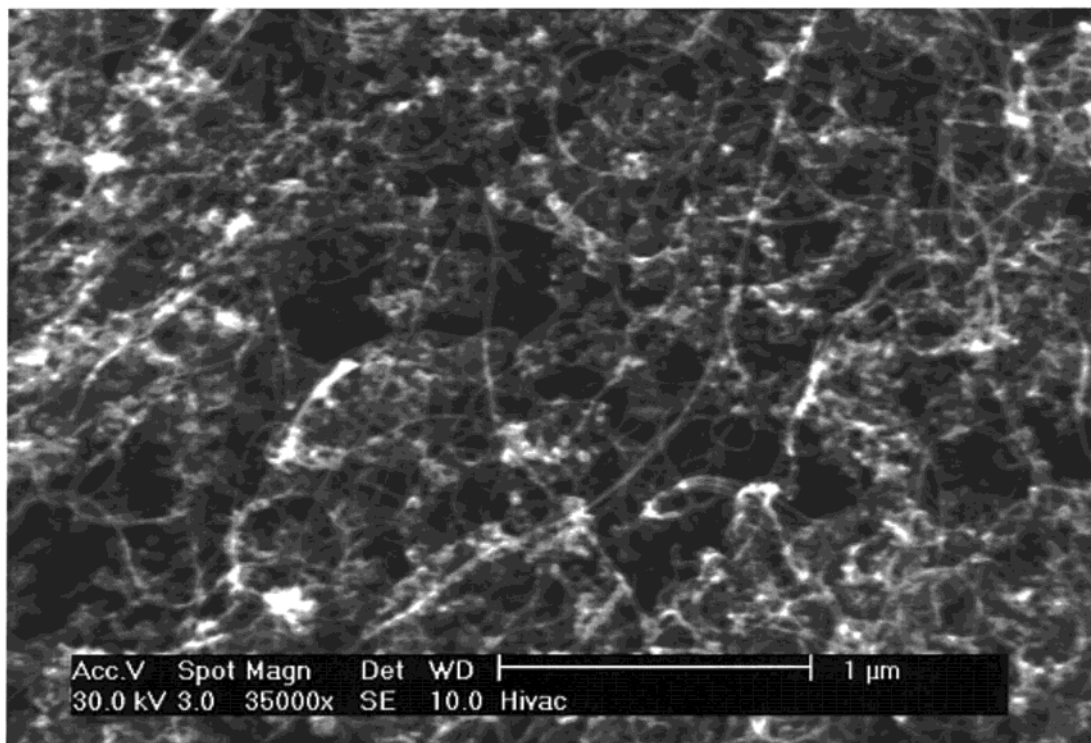


**Figure 1.** SEM of raw nanotube felt.

### Experimental Section

**Materials.** The preparation of the felt used for this report was done by the pulsed laser method, and has been described elsewhere.<sup>9</sup> The felt was stored under air in a polyethylene screw cap bottle. Graphite (Aldrich synthetic powder, 1–2  $\mu\text{m}$ ), and arc-grown single-wall nanotubes (Carbolex, AP Grade), were used as received. Approximately 5 mg of material was used for all experiments. Gases used for purification were chlorine (Scott Specialty Gases, 99.5%), hydrogen (TRIGAS, 99.99%), argon (TRIGAS, 99.998%), water from an argon bubbler, and HCl (Fisher, 12.1 M) from an argon bubbler. Solvents used include *N,N*-dimethylformamide (DMF) (ACROS, 99%), and methanol (Fisher, 99.9%). For infrared analysis the sample holder was a polyvinyl chloride gas cell with potassium bromide windows. Gases used for infrared quantitation were carbon monoxide (TRIGAS, 99%) and carbon tetrachloride (Aldrich, 99+%).

**Purification and Characterization.** The gas ratios used for purification were 7.2 mL/min  $\text{Cl}_2$ , 2.7 mL/min  $\text{H}_2$ , and 3.0 mL/min Ar bubbled through water, unless otherwise indicated. The sample was placed in a quartz tube and the system was purged, with the gases mentioned above, for 1 h at room temperature. After purging, the sample was lowered into a tube furnace at 500  $^\circ\text{C}$ , as measured by a type-K thermocouple. The evolved gases, including CO,  $\text{COCl}_2$ , and  $\text{CCl}_4$  were collected in the gas cell and monitored by infrared spectroscopy (IRS) (Perkin-Elmer, Paragon 1000PC),  $\text{CO}_2$  may also be observed at the beginning of a run, due to adsorbed gases. The reaction was carried out until the carbon monoxide partial pressure, as detected by IRS was < 0.5 Torr, unless noted. The sample was returned to room temperature, then sonicated in a 50:50 mixture of DMF:0.6 M HCl to remove metals, and then sonicated in pure DMF. The last step was filtering and methanol washing to form a paper. Alternatively the metals could be removed by sublimation in HCl at a higher temperature. The paper was dried at 160  $^\circ\text{C}$  and then weighed for yield data. The paper was characterized by SEM (Philips, EL30 ESEM-FEG), TGA (TA-Instruments Inc., SDT2960), and UV-vis (Shimadzu UV-1601PC). It should be noted that a toluene reflux and sonication was employed to remove any fullerenes that may be present after purification, but nothing was found. When not being monitored by IRS, the evolved gases were run

through an aqueous potassium hydroxide bath to remove chlorine, hydrogen chloride, and phosgene. Although not attempted here, for a larger scale process the carbon tetrachloride can be destroyed before venting, by reaction with alkaline earth metal oxides, or other methods.<sup>14</sup> Special care must be taken when working with both the reagent and product gases due to toxicity hazards, also the chlorine and hydrogen may form explosive mixtures.

### Results and Discussion

The felt produced by the laser vaporization process contains mostly other forms of carbon besides the nanotubes, including amorphous carbon and a large amount of onionated particles as shown in Figure 1. After purification, the material shows predominately nanotube ropes. Figure 2a shows the "sponge" type material after the gas-phase treatment, showing that the purification is a direct result of the gaseous chemistry and not the treatments that followed. The bright metal particles, originally cobalt and nickel catalyst, visible after the gas treatment can be removed by the DMF:HCl wash. The final paper obtained appears to be high-quality single-wall nanotube material; see Figure 2b. The difference in material quality can also be seen via UV-vis-NIR spectroscopy, as shown in Figure 3, where the unique electronic structure of the nanotubes becomes much more apparent after purification. Also the UV-vis-NIR spectrum indicates that the nanotubes are not significantly altered chemically by the purification process, and that they are electronically similar to tubes obtained by other purification techniques.<sup>15</sup> The suspension of gas-purified tubes in DMF

(14) Wekhuysen, B. M.; Mestl, G.; Rosynek, M. P.; Krawietz, T. R.; Haw, J. F.; Lunsford, J. H. *J. Phys. Chem. B* **1998**, *102*, 3773.

(15) Boul, P.; Liu, J.; Mickelson, E.; Huffman, C.; Ericson, L.; Chiang, I.; Smith, K.; Colbert, D. T.; Hauge, R.; Margrave, J.; Smalley, R. E. *Chem. Phys. Lett.* **1999**, *310* (3,4), 367.

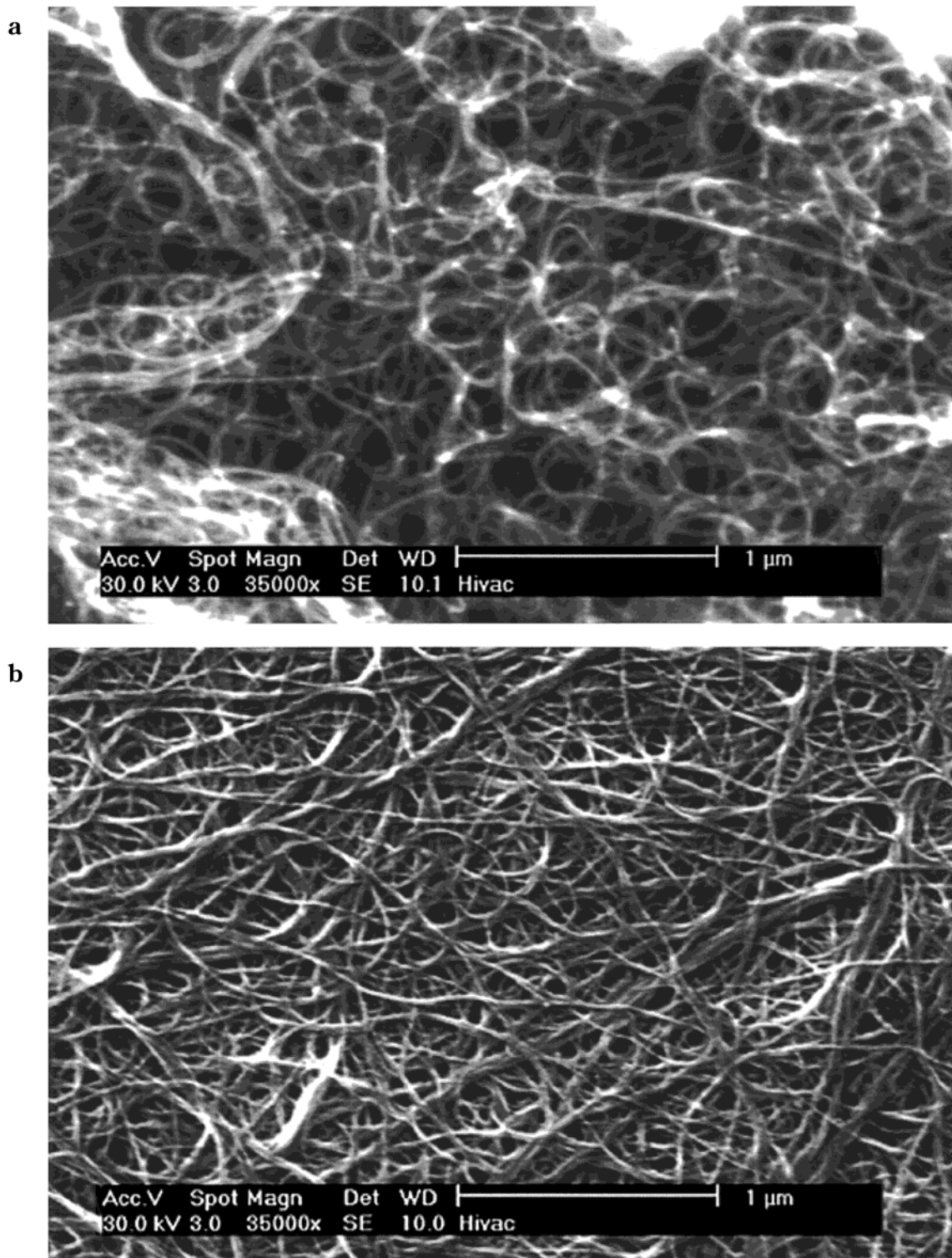


**Figure 2.** (a) SEM of gas-purified nanotube sponge and (b) SEM of gas-purified nanotubes after washing and filtering.

is limited to lower concentrations than acid-purified tubes, due to increased rope strength from the high-temperature treatment and/or residual impurities. TGA in air, Figure 4, indicated a combustion onset temperature of  $\sim 400$  °C for the purified tubes, versus  $\sim 360$  °C for the felt.<sup>9</sup> The TGA also indicates that the purified material contains  $\sim 11$  wt % of an unknown substance with a burning onset of  $\sim 235$  °C.

It is important to note the exact gas mixture that allows for purification of the nanotubes, see Table 1. Among the single component gases, chlorine is the most

effective at etching carbon, as shown by the 21% weight decrease after 6 h. There is an additional 21% weight loss when the material is subsequently washed in DMF:HCl and then filtered. The weight of the material after gas-phase water or gas-phase hydrogen chloride(aq) treatment shows no change, due to physical and chemical adsorption offsetting the small amount of carbon etched. Therefore, the IR data for the samples are needed to get a better understanding of the chemical processes responsible for carbon etching. The large weight loss exhibited with chlorine is not a result of

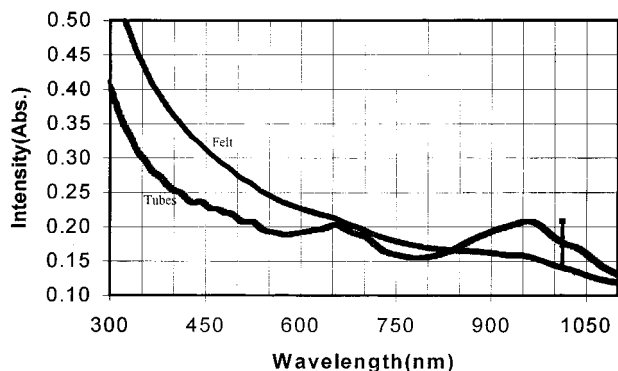


**Figure 3.** UV-vis-NIR spectra of felt and gas-purified nanotubes in DMF.

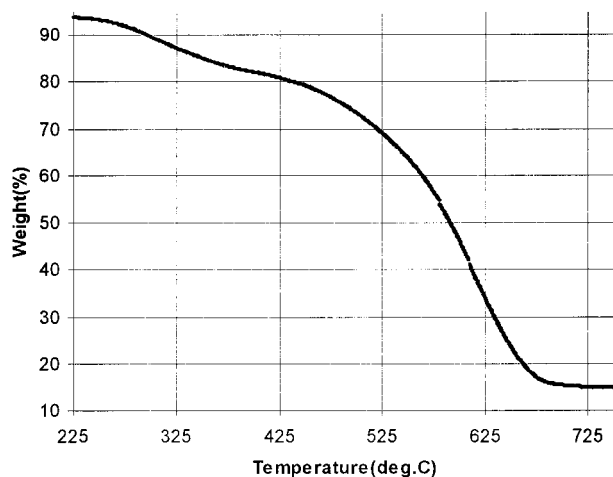


**Figure 4.** TGA in air of gas-purified tubes: 5 °C/min to 900 °C, with 1 h hold at 200 °C, 100 mL/min.

**Table 1. Summary of Control Purification Experiments for SWNT Felt<sup>a</sup>**

gas	weight change (+%/0/-%)			purification observed (y/n)
	after gas treatment	after wash and filter	total	
none	na	0	0	n
Cl <sub>2</sub>	-21	-21	-35	n
H <sub>2</sub> O	0	-12	-12	n
HCl(aq)	0	-14	-12	n
HCl(aq) + H <sub>2</sub> O <sup>b</sup>	0	-13	-18	n
Cl <sub>2</sub> + H <sub>2</sub> O	-84	na <sup>d</sup>	-84	n
Cl <sub>2</sub> + H <sub>2</sub> O <sup>c</sup>	-48	-80	-89	n
Cl <sub>2</sub> + HCl(aq)	-90	na <sup>d</sup>	-90	n
Cl <sub>2</sub> + HCl(aq) <sup>c</sup>	-77	-83	-96	y

<sup>a</sup> All reactions were for 6 h at 500 °C and flow rates 10 mL/min unless indicated. <sup>b</sup> Secondary water supply. <sup>c</sup> Bubbler flow rate = 3 mL/min <sup>d</sup> No carbon material recoverable.

direct carbon to chlorine reaction but rather the combined effect of chlorine and adsorbed air, given that infrared analysis shows that a typical carbon tetrachloride pressure is 2 orders of magnitude lower than the carbon monoxide pressure. Ultimately no single gas was found to offer any purification, or more specifically, chlorine, hydrogen chloride, or water separately do not remove carbon at a useful rate. Of the dual gas mixtures, only chlorine and water were found to remove carbon quickly. However, there is no preferential removal of unwanted carbon with just chlorine and water, and thus no purification results. The unwanted carbon is selectively removed only if hydrogen chloride is added to the chlorine and water mixture. This observation also

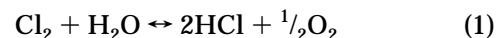
**Table 2. Nanotube Yields and Reaction Times**

conditions <sup>a</sup>	t (h)	yield (wt %)
1a (L.O.P.)	11	17.5
1b (L.O.P.)	10	16.3
2 (H.O.P.)	8.5	7.6
3 (S.O.P.)	8	11.7

<sup>a</sup> Flow rate of argon water bubbler was varied to change oxidation potential. Abbreviations: L.O.P. = low oxidation potential, flow rate = 3.0 mL/min. H.O.P. = high oxidation potential, flow rate = 5.5 mL/min. S.O.P. = stepped oxidation potential, flow rate = started at 3.0 mL/min and stepped up to H.O.P. after 2 h.

implies that the source of hydrogen chloride needs to be separate from the water to get individual control of the gas ratios, as done in this study.

It was found that the progress of the reaction could be followed by infrared spectroscopy of the effluent gas. This allows in-situ investigation of gas-phase chemistry and the ability to follow carbon etching without exposure of the sample to air. Figure 5 shows IR spectra of the gas purification products. One can clearly see the CO stretch for carbon monoxide at ~2170 cm<sup>-1</sup>, and the CCl stretch for phosgene at ~850 cm<sup>-1</sup>, and the anti-symmetric CCl stretch for carbon tetrachloride at ~792 cm<sup>-1</sup>.<sup>16</sup> As changes are made to the composition of the gas purification mixture, the results can be followed by infrared spectroscopy. The ultimate ratio of reactant gases present is determined by<sup>17</sup>



The gases introduced into the system include chlorine, water, and hydrogen chloride, which therefore determines the amount of oxygen and the overall oxidation potential toward carbon etching. The influence of water on the oxidation potential was determined for both rate of reaction and the final yield of nanotubes. Table 2 presents the results from variation of the water bubbler flow rate. With a low oxidation potential the yield of nanotubes is maximized. With inclusion of the TGA data, these values would mean 15.6% and 14.5% nanotubes respectively, which agrees well with the 10–20 wt % expected. However, this yield comes with a slow carbon etch rate and a long run time. If the oxidation potential is increased the rate of reaction can be improved, but the final yield is compromised. It was found that a stepped oxidation potential offered a little better yield and reaction rate. One explanation for this behavior is that at a high oxidation potential the heat of reaction from other carbon forms is sufficient to cause etching of nanotubes. With a stepped oxidation potential, one allows enough of the unwanted carbon to be removed before proceeding to the next level. In this case, however, it seems to indicate the need for sufficient time to remove adsorbed gases from the felt or an induction period for the establishment of the intended gas-surface interactions.

The presence of the cobalt/nickel metal catalyst in the felt could have a detrimental influence on the nanotubes. Transition metals are known to catalyze the gasification of carbon.<sup>18,19</sup> Although the exact mecha-

(16) Nakamoto, K. *Infrared and Raman Spectra of Inorganic and Coordination Compounds*, 4th ed.; John Wiley & Sons: New York, 1986.

(17) Other transient intermediates may be involved as well.

(18) Kelemen, S. R. *Appl. Surf. Sci.* **1987**, *28*, 439.

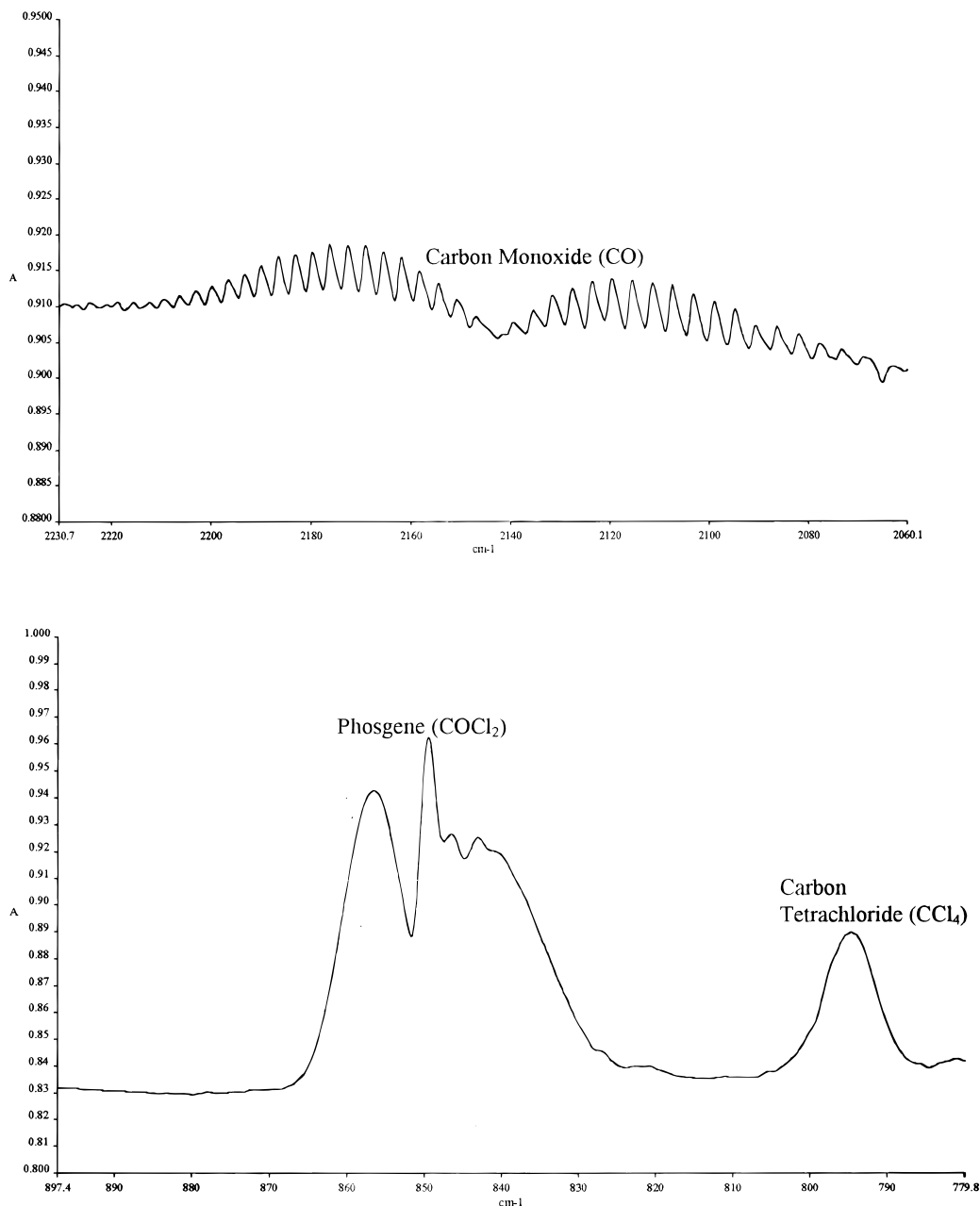


**Figure 5.** (a) IR Spectrum of carbon monoxide product gas and (b) IR spectrum of phosgene and carbon tetrachloride product gases.

nism of metal-catalyzed oxidation has been debated, as to whether gas-metal or metal-carbon interactions dominate, both interactions should be impeded by the formation of a metal chloride phase. Given that the metal catalyst is contained in a carbon shell, the interaction between the metal and the bulk of the material is not expected to be important until later in the purification process, when the metals are able to become mobile on the surface. Also the ability of chlorine on platinum to impede the catalyzed oxidation of graphite has been shown, and it is expected that the chlorine will have a similar influence on the cobalt and nickel.<sup>20</sup> With the ability to form a mixed-metal chloride-oxide phase by the gases used, interaction with the metal may become important for larger scale purifica-

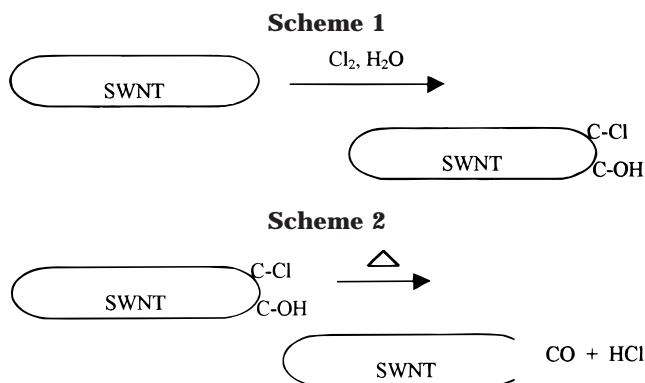
tion in which longer reaction times may be needed, or certainly whenever a higher temperature is used.<sup>21</sup>

Also of interest is the behavior of other carbon materials in the gaseous purification environment. Arc-grown single-wall nanotubes could not be purified by the same method used for the laser-grown material. The rate of carbon etching was found to drop dramatically after 3 h to a rate that was negligible. This is due to the higher density of the arc-grown material,  $\sim 0.33$  g/cm<sup>3</sup> for arc material vs  $\sim 0.03$  g/cm<sup>3</sup> for laser material, and thus a limited ability for the gases to get to reactive sites. Observation of the material after the treatment however did show an enrichment of nanotubes on the particle surface. Perhaps a high-pressure gas system could overcome the problem of decreased reaction rate. Graphite is essentially unaffected, in that there is no

(19) Pan, Z. J.; Yang, R. T. *J. Catal.* **1991**, *130*, 161.

(20) Baker, R. T. K.; Lund, C. R. F.; Dumesic, J. A. *Carbon* **1983**, *21* (5), 469.

(21) Hisham, M. W. M.; Benson, S. W. *J. Phys. Chem.* **1995**, *99*, 6194.



weight loss and the evolution of carbon gases stops completely after 1 h. This shows that the conditions used favor edge attack or defect sites for a perfectly unstrained aromatic system.

Of foremost importance in explaining the mechanism of purification is the experimental observation that hydrogen chloride is required for selective removal of unwanted carbon. As demonstrated earlier, the correct gas ratio yields a reactant mixture of low oxidation potential, which is seen to remove the impurity carbon, while leaving the nanotubes unharmed. These conditions are similar to those used by the more conventional acid purification, where the oxidation potential is controlled by acid concentration. However, the partial pressure of oxygen is still high enough for gasification of the nanotube into carbon monoxide. Even more interesting is the ability of some of the nanotubes to withstand further increases in oxidation potential. Although the nanotubes are more reactive because of the increased curvature of the graphite sheet, they do have structural features that should be of benefit, under the correct conditions. Unlike the majority of other carbon forms in the felt, the single-wall nanotubes have more perfect sidewalls, and a lack of edges due to the presence of caps. Although the caps are more reactive than the sidewall, the cap structure seems important for the nanotube survival in the gas purification environment. Schemes 1 and 2 show the plausible interactions of the chlorine gas mixture with the nanotube cap. Scheme 1 indicates the formation of a hydroxy–chloride-functionalized nanotube cap as already demonstrated in the reaction with water and carbon nanotubes and as shown in the chlorination of  $C_{60}$ .<sup>22,23</sup> These reactions illustrate the particular need for hydrogen chloride in the gas-phase purification mixture. Without the hydrogen chloride present in Scheme 2, any hydroxyl groups that form on the nanotube cap would be deprotonated, leading to the eventual breakup of the cap structure, and exposure of the strained graphitic edge. Thus, the function of the hydrogen chloride would seem to be the protection of the more reactive caps, by shifting such reactions in the reverse direction.

(22) Dillon, A. C.; Bekkedahl, T. A.; Jones, K. M.; Heben, M. J.; *FULLERENES—Recent Advances in the Physics and Chemistry of Fullerenes and Related Materials*; The Electrochemical Society: Pennington, NJ, 1996; Vol. 3, p 716.

(23) Olah, G. A.; Bucsi, I.; Lambert, C.; Aniszfeld, R.; Trivedi, N. J.; Sensharma, D. K.; Surya Prakash, G. K. *J. Am. Chem. Soc.* **1991**, *113* (24), 9385.

The various mechanisms of attack, for etching of carbon materials, offer further clarification for the survival of the more highly strained single-wall nanotubes in the purification environment. Typically the addition of a heteroatom such as oxygen, to a graphite sheet, first involves attachment at the edge, followed by desorption of the product gas. This is because the aromaticity of the basal plane does not allow attachment to the interior carbons. Likewise, the etching of a diamond also occurs at the edge of a crystal. In this case, however, it is not so much the difference in reactivity of the surface carbons in relation to the bulk, but simply that the dense packing of atoms does not allow gas species to reach the interior. Thus, the etching of diamond allows one to see the effect on reaction rate as the nature of the surface changes. The formation of a hydroxyl group on a diamond surface has been shown to offer a significant impediment to the etching rate of diamond.<sup>24</sup> In this case, the formation of a hydroxyl serves to block the etching of an oxygen environment by filling up reactive sites on the diamond surface. Because of the unique closed-cage structure of nanotubes, the formation of a hydroxyl group on the nanotube cap should also serve to protect it from oxygen attack. Unlike a planar graphite sheet with edges, a nanotube with caps only allows front-side attack, similar to diamond. This means that filling the reactive sites for front-side attack should similarly impede the action of oxygen on a nanotube. Given that the nanotube sidewall will not react under these conditions, protection of the cap means preservation of the entire tube.

Although this method has not been used on a large scale, the basic nature of gas-phase reactions should lead to a fully automated and perhaps scaleable system. With the ability to volatilize the unwanted carbon and metal chloride impurities, such a gas-phase purification represents the ultimate one step method, allowing raw material to be produced in a quartz tube and then after some time the pure nanotube “sponge” removed. The ability to preferentially remove unwanted carbon, in the presence of the more highly strained nanotubes, represents a new manner of thinking for structure–property relations of this unique material. The necessity for hydrogen chloride, in the purification gas mixture, indicates that a protection mechanism may be involved. Further work is currently underway to develop a better understanding of the role of the nanotube caps.

**Acknowledgment.** We thank Ivana Chiang, Dieter Heymann, Valery Khabashesku, Edward T. Mickelson, and Richard E. Smalley for helpful discussions and for review of the article. We also thank Fernando Rodriguez for assistance with EDAX and supply of the Carbolex material. John L. Zimmerman thanks Jelena Stanisic for helpful discussions and personal support. The financial support of the Robert A. Welch Foundation is gratefully acknowledged.

CM990693M

(24) Chu, C. J.; Pan, C.; Margrave, J. L.; Hauge, R. H. *Diamond Relat. Mater.* **1995**, *4*, 1317.